4) PHOENICS Case Studies

4.1 PHOENICS modelling of the 'Dead Water' Effect Dr R P Hornby

During his epic voyage (1893-1896) to reach the North Pole in a specially designed boat (FRAM) with a hull strong enough to withstand pack ice pressure, the Norwegian explorer Fridtjof Nansen noted some peculiar behaviour of his vessel:

'*moving at 5 knots, when the speed suddenly dropped to 1 knot and stayed that way'; 'we swept the whole sea along with us'; 'the moment the engine stopped, it seemed as if the ship was sucked back'.*

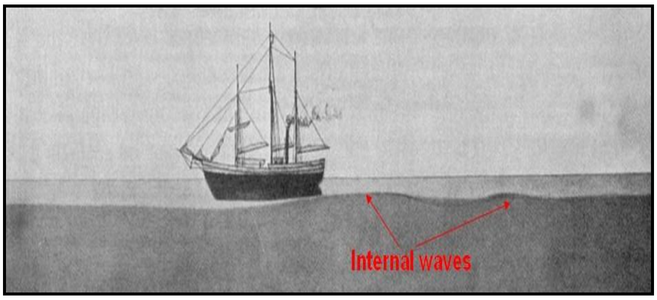

Figure 1. Ship generating internal waves on the interface between deep dense water and less dense surface water.

These effects were later shown to be due to internal wave generation (see figure 1). This is particularly pronounced in highly stratified water (Norwegian fjords, for example) when the boat speed is similar to the phase velocity of excited internal waves. When the lower, dense, water depth is much greater than the upper depth of lower density surface water, the internal wave phase velocity (in m/s) is about half the square root of the upper layer depth. So, in deep water, with an upper layer depth of 9m, the internal wave phase speed is about 1.5m/s. Mariners caught in this 'dead water' observed that the water surrounding the ship had a glassy look bounded by a turbid edge (see figure 2) and this was sometimes accompanied by a prolonged hissing sound.

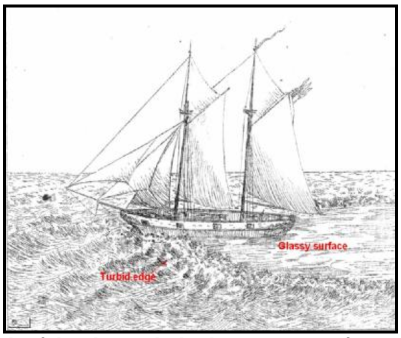

Figure 2. Sketch of the observed 'dead water' sea surface around a sailing boat: a turbid edge followed by a relatively smooth surface.

Professor Leo Maas of the Royal Netherlands Institute for Sea Research has recently hypothesised (New Scientist, December 2008) that the dead water effect could be responsible for some drowning incidents. In effect, swimmers swimming in stratified waters (deep lakes in summer, fjords, river outflows into the sea) could find a significant percentage of their propulsive power used to generate internal waves rather than forward motion – resulting in fatigue and drowning.

In order more clearly to understand the dead water effect, a series of experiments have been conducted at the Royal Netherlands Institute for Sea Research, starting with model boat experiments and culminating with experiments comparing swimming times in homogenous and stratified water. PHOENICS is being used to model these flows and compare with experimental results. Initially a 3-D transient model has been developed which couples the boat motion (determined by the boat propulsive thrust and the fluid drag) to the fluid flow. Figure 3 shows a comparison between the PHOENICS predictions and the experiment (which lasted about 20s) for a 'rectangular' boat shape.

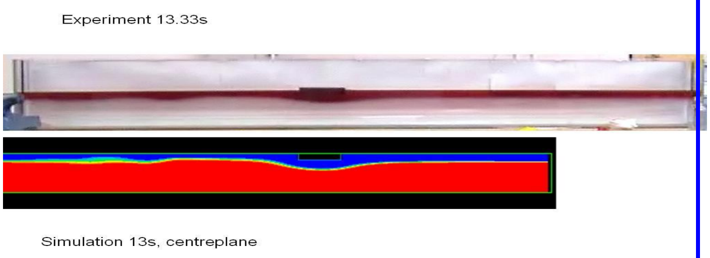

Figure 3. Comparison of experiment (top) at 13.33s and the PHOENICS simulation at 13s for a rectangular boat shape. In the experiment the upper less dense layer is dyed red and overlays denser fluid (no dye). In the PHOENICS simulation the less dense fluid is coloured blue and the dense fluid coloured red. The boat is travelling from left to right.

The PHOENICS result is very encouraging, illustrating the essential interfacial wave characteristics well.

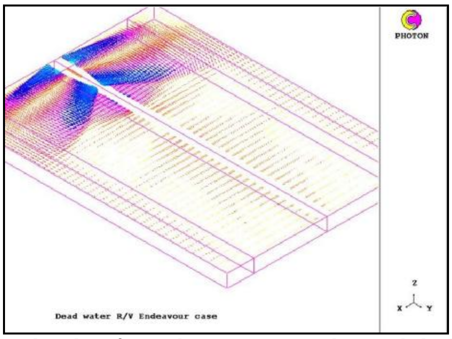

Figure 4. Predicted surface velocity vectors (colour coded) showing the presence of bow and stern, near transverse, attached, internal waves.

A full scale simulation has also been carried for a 56m length, 5m beam, 3.8m draft vessel with a displacement of 1000 tons moving at 0.9m/s in open water with an upper layer depth of 4m. For this case a wave absorbing region has been incorporated on the extremities of the lateral boundary to avoid non-physical wave reflections. The results for the surface velocity vectors are shown in figure 4. The principal features are attached, near transverse, bow and stern internal waves.

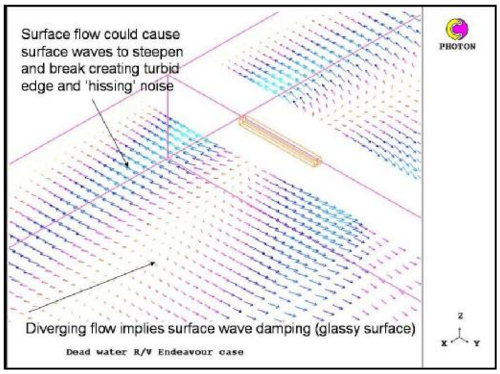

Figure 5. Close up view of near field surface flow vectors (colour coded) showing circulations of opposite sign in the bow and stern internal waves.

Figure 5 shows a close up of the near field surface velocity vectors showing that the waves at bow and stern have opposite circulation. This means that the region between these waves is a region of flow divergence which will tend to suppress surface waves. This is a possible explanation for the observed 'glassy' surface. Also the flow convergence at the head of the bow internal wave will promote surface waves which in certain circumstances may break causing a 'hissing' sound.

Future work will firstly concentrate on the effect of background internal waves on the boat motion. Ultimately, the flow created by a swimmer will be modelled using some of the more advanced PHOENICS features and results compared with the experiments at the Royal Netherlands Institute for Sea Research.

Dr R P Hornby e-mail: bob@hornby007.wanadoo.co.uk

3) PHOENICS Applications

3.1 Is Swimming in Stratified Water Safe? by Bob Hornby

It has recently been hypothesised (New Scientist, December 2008) that stratification in lakes or the sea could be responsible for some of the 400,000 drowning incidents that occur each year (WHO 2002, Peden and McGee 2003, Inj Control Saf Promot 10:195-199). The article suggests that swimmers swimming in stratified waters (deep lakes in summer, fjords, river outflows into the sea) could find a significant percentage of their propulsive power used to generate internal waves rather than forward motion – resulting in fatigue and drowning.

This realisation has followed on from experimental investigations (using model boats) of the 'Dead water effect' which is known to considerably slow the motion of ships moving at low speeds in stratified waters (see PHOENICS Newsletter Spring 2009). It has been supported by further experiments (Sander et al 2008, Naturwissenschaften), in particular, *'where four subjects swam a short distance (5m) in homogeneous and in two different settings of stratified water. At the same stroke frequency swimming in stratified water was slower by 15% implying a loss in propulsive power of 40%.'*

PHOENICS modelling of the initial model boat experiments showed encouraging agreement and this has prompted the current more complex work to use PHOENICS to model the motion of a swimmer and to gain further understanding of the experimental findings. This requires the additional effect of the motion of arms and legs relative to the body to be determined.

For homogeneous flow, a simple mathematical model of the swimmer motion can be constructed (see figure 1). It is sufficient to consider a single arm motion as the second arm and two leg motions follow using the same analysis method.

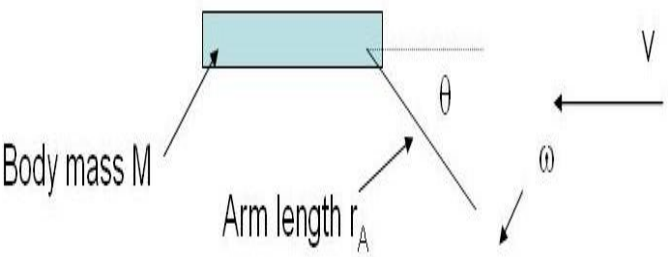

Figure 1. Schematic for a swimmer of mass M moving at velocity v from left to right (taken as positive y direction, with z measured vertically and x positive out of page) with arms rotating with angular velocity ω

The propulsive force on the swimmer minus the drag force is equal to the body mass multiplied by the body acceleration. The drag force due to just the body section can be written as

$$\frac{1}{2} c_B \rho v^2 A_B$$

Where c_B is the body drag coefficient, ρ is the fluid density, v the approach velocity (considering a reference frame with the swimmer body at rest) and A_B the body area normal to the flow direction..
The arms and legs contribute a propulsive force where the local arm/leg velocity is larger than v and a drag effect elsewhere.

For example, the axial arm force due to an element length dr of arm is:-

$$c_A \frac{1}{2} \rho(-\omega r + v\sin\theta)\left|-\omega r + v\sin\theta\right| b_A \sin\theta dr$$

Where ω is the arm angular velocity, c_A is the drag coefficient for the arm and b_A is the arm width. Note that this expression has been adjusted, for convenience, so that the values of ω, θ and v are positive.

Integrating this over an arm length and then incorporating the body drag force as above gives the equation of motion for a body propelled by two arms with a half cycle phase difference.

$$M\frac{dv}{dt} = \frac{1}{2} c_A \rho b_A \left(v^2 r_A \sin^3\theta - \omega v r_A^2 \sin^2\theta + \frac{1}{3}\omega^2 r_A^3 \sin\theta - \frac{2}{3}\frac{v^3 \sin^4\theta}{\omega}\right) - \frac{1}{2} c_B \rho v^2 A_B$$

A similar equation can be derived incorporating the leg motions.

A swimmer is modelled by PHOENICS in a reference frame at rest with respect to the body. This requires a uniform inflow velocity equal to the swimmer speed and an axial body force applied throughout the flow proportional to the swimmer acceleration. The ambient hydrostatic pressure distribution has been found to be a satisfactory outlet boundary condition. Other flow boundaries are assumed to be frictionless.

The body and head are represented simply by rectangular, solid, frictionless objects. Figure 2 gives the body dimensions used as well as other modelling dimensions which are representative of the experiments. The effect of arms and legs is represented by moving momentum sources as described below. A non-uniform Cartesian grid is used with 38 cells in the lateral direction 104 cells in the axial direction and 32 cells in the vertical direction with due regard to concentration of cells in regions of large gradient. Eighty time steps are used per swimmer stroke and four strokes are usually sufficient to achieve a near steady state.

A strong stratification (density 1000.0 kg/m^3 in the upper layer and 1025 kg/m^3 in the lower layer) is employed as in the experiments.

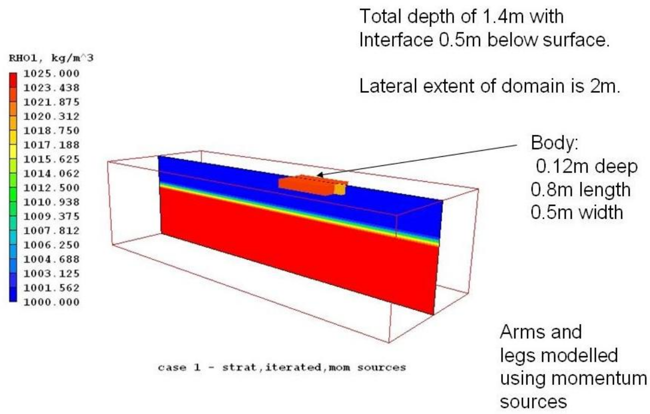

Figure 2. Dimensional modelling details for the PHOENICS simulation with x measured laterally out of the page, y in the swimmer direction and z vertically.

The equations to be solved by PHOENICS are as shown in figure 3 (using standard notation). The enthalpy equation is used to represent density transport. Sources are shown as subscripted S terms. F is the total propulsive force to the swimmer from arm and leg motions and D is the total drag from body, arms and legs. M is the total mass of the swimmer, taken as 70kg. A laminar viscosity is employed in this exploratory analysis but turbulence effects could be represented using one of the standard PHOENICS turbulence models. Note however, that turbulence effects are implicitly represented, in part, by use of appropriate drag coefficients for arms and legs. The drag due to the body section alone is computed from the pressure forces acting on the front and rear faces of the body and the friction force on the lower surface.

The arms and legs are assigned specific motions (for example arms rotating at a fixed angular velocity with a phase difference of π). Arms and legs are represented as thin plates, the arms with length 0.7m and width 0.1m and the legs with length 1m and width 0.1m.. Each arm and leg is then subdivided into n by m panels where n is the number of panels across the width and m the number of panels along the length. The values of n and m can be different for arm and leg.

At each time step, the coordinates of the centre of each panel are calculated and the panel velocity calculated there. Figure 4 shows a snapshot of the arm and leg positions so determined using a marker variable MARK. The centre of each panel is then associated with the PHOENICS flow cell in which it resides. For example, for each arm, the fluid force contribution of this panel to the axial and vertical momentum source terms is respectively

$$c_A \frac{1}{2}\rho(-\omega r + v\sin\theta)\left|-\omega r + v\sin\theta\right|\sin\theta dA$$

and

$$-c_A \frac{1}{2}\rho(-\omega r + v\sin\theta)\left|-\omega r + v\sin\theta\right|\cos\theta dA$$

where dA is the panel area, r the radial distance of the panel centre from the arm pivot point and θ the angle the arm makes with the horizontal (figure 1). The legs are treated similarly. Note that these expressions have been adjusted, for convenience, so that the values of ω, θ and v are positive.

These contributions are summed for all the arm and leg panels. The negative of the axial fluid force is used in the equation of motion for the body which is solved iteratively in conjunction with the fluid motion.

Figure 3. Equations solved by PHOENICS with boundary conditions

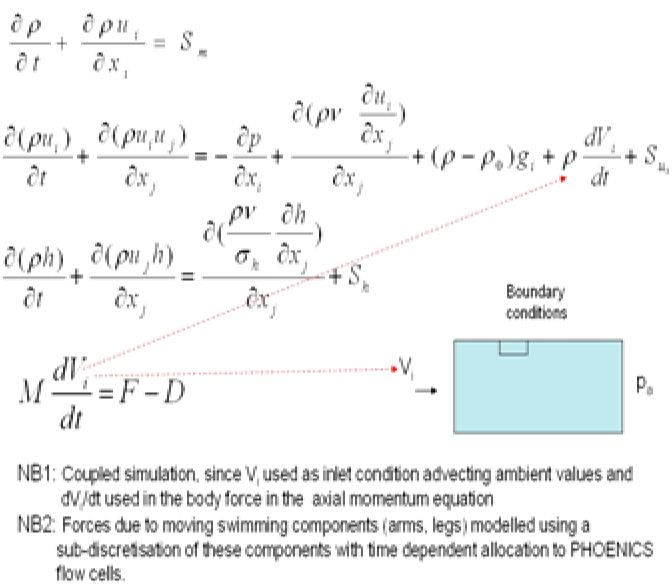

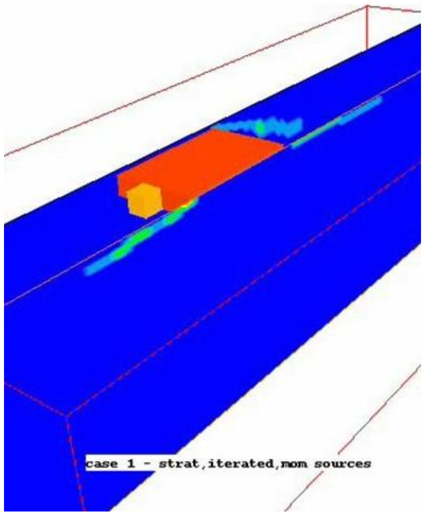

Figure 4. A snapshot of arm and leg movements shown using the MARK tracer. Note that the second arm is not visible because it is out of the water.

The PHOENICS coding to achieve the coupled simulation with moving momentum sources is fairly complicated so this was tested by comparing a PHOENICS run for a 2s stoke in homogeneous water with the mathematical model described above when the body drag component is set to zero (drag coefficients for arms and legs are set equal to 1.0). For this case the mathematical model and PHOENICS should agree exactly apart from errors associated with the subdivision of arms and legs (which should reduce as n and m, the subdivision parameters, increase). The results given in figure 5, for a swimmer starting from rest, show excellent agreement. But this figure also shows that there is no significant difference between the homogeneous PHOENICS run and a further run with the stratification profile shown in figure 1. This is a surprising result given the experimental findings.

Further PHOENICS runs for homogeneous and stratified water (parameters as above) which include the body drag term again show negligible difference. This is shown in figure 6, which also shows reasonable agreement with the mathematical model when a feasible body drag coefficient (0.4) is assumed.

Additional PHOENICS runs varying the stroke period and the upper layer depth for the stratified case also show insignificant difference between the stratified and homogeneous cases.

Hence the conclusion from the PHOENICS simulations is that swimming speed is NOT significantly affected by stratification. For the stratified cases, the simulations show no effect of the swimmer body on the density interface. For ships the hull interacts strongly with the density interface producing a deep broad wave which significantly affects the pressure distribution around the boat and therefore the drag. The swimming body has too little depth to produce an equivalent effect and the hands produce only a narrow wave that carries little energy.

This can be illustrated with the following simple calculation. A 70kg swimmer moving at $1 ms^{-1}$ has kinetic energy of 35 J. The potential energy as each hand moves a differential mass of fluid, δm, through distance h is

$$\delta mgh$$

where g is acceleration due to gravity. Over n swimming strokes this energy sums to

$$2n\delta mgh$$

where 1 stroke involves a complete hand cycle.

In the preceding analysis about 4 strokes were required to reach a steady speed so take n=4. From the simulations, h is about 0.1m (the internal wave height) and the 'handful' of differential mass raised is estimated at 0.1kg.

This gives the potential energy associated with the internal waves created as 0.8J, small in comparison with the kinetic energy attained by the swimmer.

The conclusions from the simulations are therefore different to those from the experiments where a significant difference (reduction) in speed was attained when swimming in stratified water. Normally the experimental results would be given more credence, but then the difficulty in producing equivalent swimming actions in homogeneous and stratified water must be accepted. Or perhaps some subtle effect in the modelling has been overlooked?

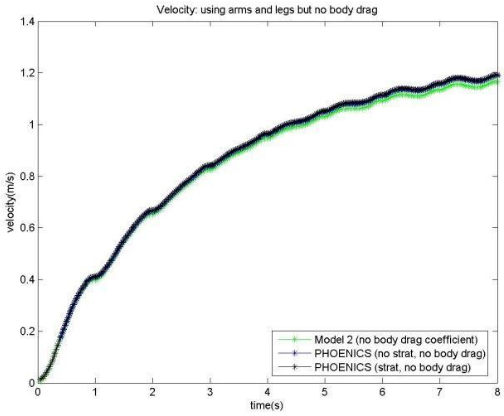

Figure 5. Comparison of PHOENICS results for homogeneous and stratified water for a swimmer starting from rest with a 2s swimming stroke. No body drag is included.

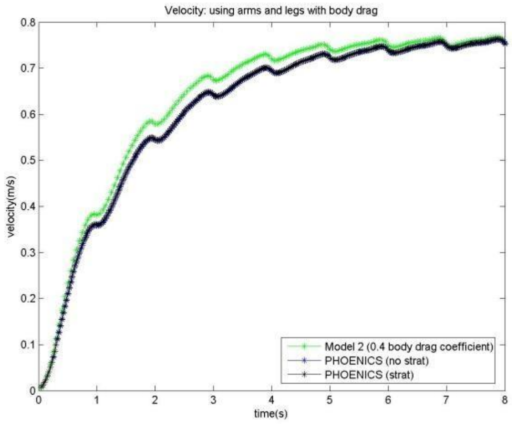

Figure 6. Comparison of PHOENICS results for homogeneous and stratified water for a swimmer starting from rest with a 2s swimming stroke. Body drag is included.